

Multiple Bosonic Mode Coupling in Electron Self-Energy of $(La_{2-x}Sr_x)CuO_4$

X. J. Zhou^{1,2}, Junren Shi³, T. Yoshida^{1,4}, T. Cuk¹, W. L. Yang^{1,2}, V. Brouet^{1,2}, J. Nakamura¹, N. Mannella^{1,2}, Seiki Komiya⁵, Yoichi Ando⁵, F. Zhou⁶, W. X. Ti⁶, J. W. Xiong⁶, Z. X. Zhao⁶, T. Sasagawa^{1,7}, T. Kakeshita⁸, H. Eisaki^{1,8}, S. Uchida⁸, A. Fujimori⁴, Zhenyu Zhang^{3,9}, E. W. Plummer^{3,9}, R. B. Laughlin¹, Z. Hussain², and Z.-X. Shen¹

¹Dept. of Physics, Applied Physics and Stanford Synchrotron Radiation Laboratory, Stanford University, Stanford, CA 94305

²Advanced Light Source, Lawrence Berkeley National Lab, Berkeley, CA 94720

³Condensed Matter Sciences Division, Oak Ridge National Laboratory, Oak Ridge, TN 37831

⁴Department of Complexity Science and Engineering,
University of Tokyo, Kashiwa, Chiba 277-856, Japan

⁵Central Research Institute of Electric Power Industry,
2-11-1 Iwato-kita, Komae, Tokyo 201-8511, Japan

⁶National Lab for Superconductivity, Institute of Physics,
Chinese Academy of Sciences, Beijing 100080, China

⁷Department of Advanced Materials Science, University of Tokyo, Japan

⁸Dept. of Superconductivity, University of Tokyo, Bunkyo-ku, Tokyo 113, Japan

⁹Department of Physics and Astronomy, University of Tennessee, Knoxville, TN 37996

(Dated: November 1, 2018)

High resolution angle-resolved photoemission spectroscopy data with significantly improved statistics reveal fine structure in the electron self-energy of the underdoped $(La_{2-x}Sr_x)CuO_4$ ($x=0.03$, 0.063 and 0.07) samples in the normal state. Four fine structure have been identified near 27 , 45 , 61 and 75 meV. These features show good correspondence to the structure in the phonon density of states as measured from neutron scattering.

PACS numbers: 74.25.Jb, 71.18.+y, 74.72.Dn, 79.60.-i

The recent observation of the electron self-energy renormalization effect in the form of a “kink” in the dispersion has generated considerable interest because it reveals a coupling of the electrons with a collective boson mode of the cuprate superconductors[1]. However, the nature of the bosons involved remains controversial mainly because the previous experiments can only be used to determine an approximate energy of the mode and this energy is close to both the optical phonon[2, 3] and the spin resonance[4]. Determining the nature of the mode(s) that couple to the electrons is likely important in understanding the pairing mechanism of superconductivity.

In conventional superconductors, identification of the fine structure for the phonon anomalies in the tunnelling spectra has played a decisive role in reaching a consensus on the nature of the bosons involved[5]. The fine structure provides fingerprints for much more stringent comparison with known boson spectra. So far, such fine structure has not been detected in the angle-resolved photoemission spectroscopy (ARPES) data. In this Letter we present significantly improved high resolution ARPES data of $(La_{2-x}Sr_x)CuO_4$ (LSCO) that, for the first time, reveal fine structure in the electron self-energy, demonstrating the involvement of multiple boson modes. We identify four bosonic modes that couple to the electrons and the energies of the modes are near 27 , 45 , 61 and 75 meV. This fine structure corresponds to some known phonon features in this material.

The photoemission measurements were carried out on beamline 10.0.1 at the ALS, using a Scienta 2002 electron

energy analyzer. As the real part of electron self-energy is already a small effect, high energy resolution and high data statistics are necessary to investigate its fine structure. The experimental conditions are set to compromise between these two conflicting requirements. The photon energy is 55 eV and the energy and angular resolutions are $18\sim20$ meV and 0.3 degree, respectively(see [3] for details). An example of the high quality of the raw data is shown in Figs. 1a and 1b. Due to space charge problem, the Fermi level calibration has a ± 2.5 meV uncertainty. We mainly present our data on the heavily underdoped LSCO $x=0.03$ (non-superconducting), LSCO $x=0.063$ ($T_c=12$ K) and LSCO $x=0.07$ ($T_c=14$ K) samples. The heavily underdoped LSCO samples are best candidates because they exhibit a stronger band renormalization effect[3]; a relatively large magnitude of the real self-energy makes the identification of the fine structure easier. The LSCO single crystals are grown by the travelling solvent floating zone method[7]. The samples were cleaved *in situ* in vacuum with a base pressure better than 4×10^{-11} Torr. The measurement temperature was ~ 20 K so all samples were measured in the normal state.

We have used the MDC method to extract the energy-momentum dispersion relation (Fig. 1c). We chose to measure the dispersion along the nodal direction because this is technically the most reliable direction to get high quality dispersion data using the momentum distribution curves (MDC). It has been shown theoretically that this approach is reasonable in spite of the momentum-dependent coupling if we are only interested in identify-

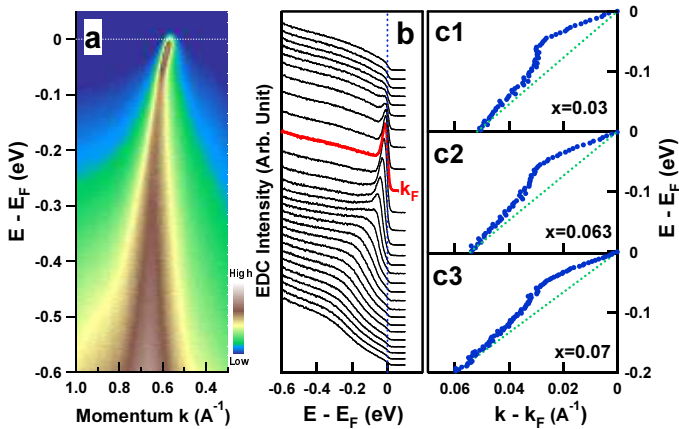


FIG. 1: (a) Typical raw data of a two-dimensional image showing the photoelectron intensity as a function of the momentum and energy for the LSCO $x=0.063$ sample. The intensity is expressed by the false-color. The measurement was taken along the $(0,0)$ - (π,π) nodal direction and at a temperature of 20 K. (b) The photoemission spectra (energy distribution curves, EDCs) for the LSCO $x=0.063$ sample corresponding to Fig. 1a. The spectrum at the Fermi momentum $k_F=(0.44\pi/a, 0.44\pi/a)$ (red curve) shows a sharp peak. (c) The energy-momentum dispersion for LSCO $x=0.03$ (c1), $x=0.063$ (c2) and $x=0.07$ (c3) samples, as determined from fitting the MDCs. The green dashed lines connecting the two points at the Fermi energy and -0.2 eV are examples of a simple selection of the bare band.

ing the mode energies[6]. In Fig. 1c, there is a clear break in slope (“kink”) in all the $(0,0)$ - (π,π) nodal dispersions for the LSCO with various doping levels, as previously reported [3]. However, the improved statistics of the data indicates that the “kink” has fine structure and subtle curvatures in it. Since the bare dispersion is expected to be smooth in such a small energy window, the “kink” and its fine structure represent effects in the electron self-energy.

Having identified the self-energy anomalies in the raw dispersion data, the next step is to extract the self-energy $\text{Re}\Sigma$ by subtracting the “bare dispersion” of the quasi-particle. We start our analysis with an empirical approach by following the convention and assume the “bare band” within a small energy range near the Fermi level as $\epsilon_0(k)=a_1(k-k_F)+a_2(k-k_F)^2$ [8, 9]. As we will describe later, the values of a_1 and a_2 are determined so as to yield the best fit of the measured dispersion (Fig. 1c) from the maximum entropy method (MEM) and the choice of a smooth bare band has little effect on the fine structure that originates from the abrupt change in the dispersion. The “effective” real part of the electron self-energy for LSCO at various doping levels is shown in Fig. 2a where the error bar increases with increasing binding energy as in Fig. 3a. The data in Fig. 2a2 were collected with a slightly better energy resolution (~ 15 meV) and a smaller

energy step (1 meV) at the expense of statistics.

As seen from Fig. 2a, even with our optimal experimental conditions and in the samples that exhibit the largest self-energy effects, there remains considerable noise in the data. However, by searching for peaks or curvature changes, we can clearly identify some fine structure in the data. The first one is near 27 meV, which shows up mainly as a shoulder that appear more clearly for $x=0.03$ (Fig. 2a1) and 0.07 (Fig. 2a4); indications of the feature are also seen in another $x=0.03$ sample (Fig. 2a2) and $x=0.063$ sample (Fig. 2a3) although they are less clear. The other two structure are near 45 meV and 61 meV which show up more clearly in $x=0.03$ (Fig. 2a1 and 2a2) and less clearly in $x=0.063$ and $x=0.07$ samples. While the fine structure is subtle and one may argue about individual curves, we have invariably observed them near similar energies in many independent measurements. The measurements of different dopings make the presence of the fine structure convincing and consistent.

A natural question is whether the fine structure can be due to instrumental artifact which may be related to detector inhomogeneity and/or system noise. The possibility of detector problem can be ruled out because the data were taken using the “swept mode” of the electron analyzer, i.e., each energy point was averaged over the entire detector range along the energy direction. Therefore, all the energy points were taken under the same condition, independent of the detector inhomogeneity. The possibility of noise problem can also be ruled out because they are supposed to be random while for different samples, under different experimental conditions such as different photon energies and different pass energies of the analyzer (Fig. 2a1 and 2a2), the multiple structures are all invariant in binding energy.

The existence of fine structure indicates the involvement of several collective modes in the coupling, with each structure representing a “subkink” in the dispersion and defining the energy scale of the mode. We quantify the characteristic energies by fitting a smooth curve through the $\text{Re}\Sigma$ data and then performing second-order derivative to the fitted curve. Given the noise level in the data, a spline through the data is difficult and somewhat subjective. To this end, we first use the MEM procedure which has been exploited to extract the spectral features of the electron-phonon coupling from ARPES data for the two-dimensional surface state of Be[9]. Since *a priori* we do not know whether the method developed for conventional metal can be extended to cuprate superconductors, we use it only as the first step a procedure for systematic curve fitting. The MEM is more objective in getting the fine structure because the number of peaks and their positions are insensitive to the fitting details[9].

The fitted curves are shown in Fig. 2a together with the measured $\text{Re}\Sigma$. In Fig 2b, we show the second-order derivative of the fitted curves whose peaks reveal the energies of the collective modes. As expected, the

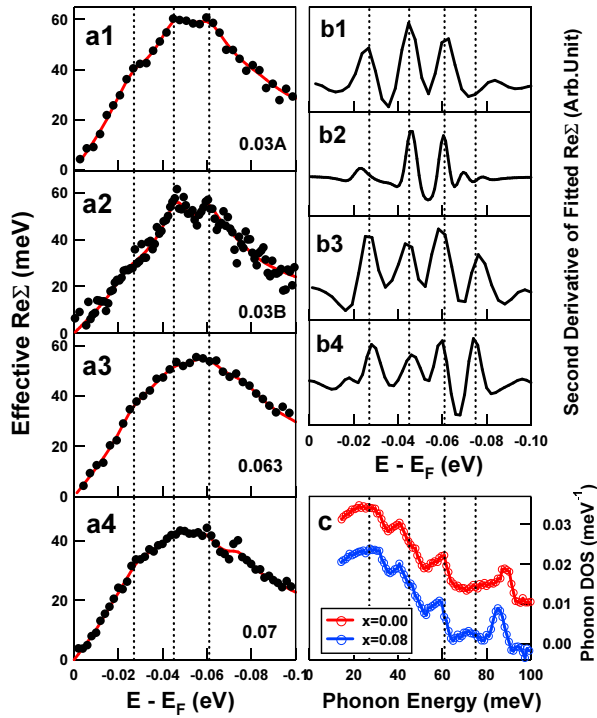


FIG. 2: (a).The effective real part of the electron self-energy for LSCO $x=0.03$ (a1), 0.03 (a2), 0.063 (a3) and 0.07 (a4). The data on (a2) were obtained on a separate $x=0.03$ sample using 5 eV pass energy of the electron analyzer in order to take advantage of a smaller energy step (1 meV) while the others were all taken with 10 eV pass energy and a larger energy step. The bare bands were assumed as $\epsilon_0(k)=a_1(k-k_F)+a_2(k-k_F)^2$ (the unit of a_1 and a_2 are $\text{eV}\cdot\text{\AA}$ and $\text{eV}\cdot\text{\AA}^2$, respectively) with $a_1=-4.25$, $a_2=0$ for (a1), $a_1=-6.8$, $a_2=-10$ for (a2), $a_1=-4.25$, $a_2=13$ for (a3), and $a_1=-3.7$, $a_2=7$ for (a4). The solid red lines are calculated from the extracted effective bosonic function using the maximum entropy method. (b). The second-order derivative of the calculated $\text{Re}\Sigma$. The ruggedness in the curves is due to limited discrete data points. The four dashed lines correspond to energies of 27, 45, 61 and 75 meV. (c) The phonon density of state $F(\omega)$ for LSCO $x=0$ (red) and $x=0.08$ (blue) measured from neutron scattering[12]. The four vertical lines correspond to the same energies as in Fig. 2b.

peaks correspond to anomalies in the raw data. Three main features near 27, 45 and 61 meV can be resolved for different samples with different doping levels, consistent with the fine structure visible to a naked eye in the electron self-energy (Fig. 2a). Again, the consistency and the robustness of the energy scales in all the data sets give credence to these three energy scales revealed. In addition, the MEM procedure has resulted in one more possible feature between 70 and 80 meV which appears stronger with increasing doping[10].

The existence of fine structure in the electron self-energy indicates that there must be fine structure present in the underlying bosonic spectral function. The identified multiple sharp features (Fig. 2b) are different from

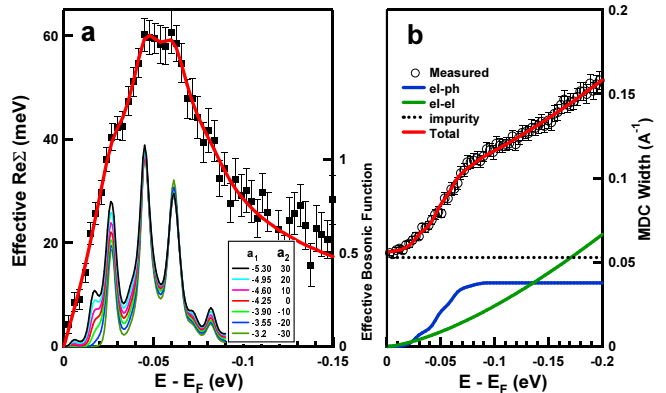


FIG. 3: (a)Real part of the electron self-energy for LSCO $x=0.03$ as obtained from the dispersion shown in Fig. 1c1 (solid square) and calculated from the extracted effective bosonic spectral function using the MEM procedure (red solid curve) with $a_1=-4.25$ and $a_2=0$. Also plotted are the effective bosonic functions obtained by using different bare bands as represented by the different sets of a_1 and a_2 values. (b) The MDC width of LSCO $x=0.03$ (open circles). The contribution from the electron-phonon coupling (blue line) is calculated from the effective bosonic function in Fig. 3a with $a_1=-4.25$ and $a_2=0$. The “impurity” contribution is assumed to be a constant (dotted black line). The momentum resolution here is 0.019 \AA^{-1} . After subtracting all the electron-phonon and “impurity” contributions, the residual part is proportional to ω^α ($\alpha\sim 1.5$) (green line).

the magnetic excitation spectra measured in LSCO from neutron scattering[11]. On the other hand, the first three features (Fig. 2b) show close correspondence to the three low-energy features in the phonon density-of-states (DOS), measured also from neutron scattering on LSCO (Fig. 2c)[12]. We do not see the strong phonon feature near 85~90 meV but we observe a feature near 75 meV which appears to get more pronounced at higher doping. This is consistent with the known result that the full-breathing phonon mode near 85~90 meV shows much weaker doping-induced change, indicating a weaker coupling, than the anomalous doping-induced softening of the half-breathing mode from 80 meV to 70 meV (see the new peak near 75 meV for $x=0.08$ in Fig. 2b), indicating a much stronger coupling[12]. The good correspondence between the extracted fine structure and the measured phonon features provides further evidence that the bosons involved in the coupling are phonons. In addition to the half-breathing mode at 70~80 meV that we previously considered strongly coupled to electrons[2], the present results reveal that several lower energy optical phonons of oxygens are also actively involved. This means that the observed renormalization has several contributions so that the quantitative value of the coupling strength should not be attributed to the highest energy of the breathing mode alone.

For conventional metals, the MEM procedure can be

used to extract the Eliashberg function which gives spectral features of the electron-phonon coupling[9]. For strongly correlated cuprate superconductors, *a priori* it is unclear whether the Eliashberg formalism is applicable or not. However, we note that the nodal excitation of LSCO in the normal state may provide a closest case for the procedure to be applicable. Recent transport measurements reveal that a quasiparticle picture may be still reasonable for electrons near the nodal direction, even for very low doping[13]. This is consistent with the ARPES data which show a well-defined peak in the nodal spectra in the lightly doped samples[3]. The nodal dispersion does not have pronounced structure in its bare band, unlike the strong curvature near the saddle point of the antinodal region. The selection of the nodal direction in the normal state also minimizes complications due to the existence of a superconducting gap or pseudogap in the extraction process.

Given these considerations and the fact that there is no better alternative available, we have applied the Eliashberg formalism and the MEM procedure to extract the effective bosonic function from the real part of the electron self-energy (Fig. 3a). It is clear that the multiple features are rather robust against the choice of the bare band by varying a_1 and a_2 . All other tests as detailed in [9] have been carried out. The fine structure as obtained from LSCO $x=0.03$ is in agreement with that in the second-order derivative shown in Fig. 2b. The calculated real part of the electron self-energy is plotted in Fig. 3a together with the measured data. Fig. 3b shows the MDC width which is directly related to $\text{Im}\Sigma=(\Gamma/2)v_0$, with Γ being the MDC width (Full-Width-at-Half-Maximum, FWHM) and v_0 the bare velocity. While there is a drop near 75 meV, there is an overall increase of the MDC width with increasing binding energy (Fig. 3b), which is different from simple electron-phonon coupling systems such as Be[8]. The MEM analysis allows us to calculate the abrupt drop in $\text{Im}\Sigma$ which is due to electron-phonon coupling. After subtracting the contributions from the electron-phonon coupling, “impurity” scattering, and angular resolution, the residual part is found to be proportional to ω^α ($\alpha\sim 1.5$)(Fig. 3b). This term most likely represents the contribution of the electron-electron interaction. The corresponding electron-electron contribution in the real part of the self-energy is a smooth function and may be absorbed into the “bare dispersion” because we focus only on abrupt structure in $\text{Re}\Sigma$ in extracting the bosonic spectral function. Here we also note that while the imaginary part of the electron self-energy is consistent with the existence of electron-phonon coupling, it is difficult to identify the fine structure as has been done for the real part because of the larger experimental uncertainty in determining the peak width over the peak position. This analysis also shows that there is an internal consistency in the MEM procedure that connects the real and imaginary parts of the self-energy.

In summary, by taking high resolution data on heavily underdoped LSCO samples with high statistics, we have detected fine structure from multiple bosonic coupling in the electron self-energy near 27, 45, 61 and 75 meV.

The work at the ALS and SSRL is supported by the DOE’s Office of BES, Division of Material Science, with contract DE-FG03-01ER45929-A001. The work at Stanford was also supported by NSF grant DMR-0304981 and ONR grant N00014-98-1-0195-P0007. EWP was supported by NSF grant DMR 0105232. The work at Oak Ridge National Laboratory was partially supported through DOE under Contract DE-AC05-00OR22725. The work in Japan is supported by a Grant-in-Aid from the Ministry of Education, Culture, Sports, Science and Technology of Japan and the NEDO. The work in China is supported by NSF of China and Ministry of Science and Technology of China through Project 10174090 and Project G1999064601.

- [1] A. Damascelli, Z.-X. Shen and Z. Hussain, Rev. Mod. Phys. **75** (2003) 473.
- [2] A. Lanzara et al., Nature (London) **412**, 510(2001).
- [3] X. J. Zhou et al., Nature (London) **423**, 398 (2003); X. J. Zhou, et al., Phys. Rev. Lett. **92**, 187001(2004); T. Yoshida et al., Phys. Rev. Lett. **91**, 027001 (2003).
- [4] A. Kaminski et al., Phys. Rev. Lett. **86**, 1070 (2001); P. D. Johnson et al., Phys. Rev. Lett. **87**, 177007 (2001); S. V. Borisenko et al., Phys. Rev. Lett. **90**, 207001 (2003).
- [5] J. M. Rowell et al., Phys. Rev. Lett. **10**, 334 (1963); D. J. Scalapino et al., Phys. Rev. **148**, 263 (1966).
- [6] A. W. Sandvik et al., cond-mat/0309171; T. P. Devereaux et al., cond-mat/0403766.
- [7] S. Komiya et al., Phys. Rev. B **65**, 214535 (2002); F. Zhou et al., Supercon. Sci. Technol. **16**, L7 (2003).
- [8] S. Lashell et al., Phys. Rev. B **61**, 2371(2000).
- [9] J. R. Shi et al., Phys. Rev. Lett. **92**, 186401 (2004).
- [10] For the LSCO $x=0.07$ sample, the peak at 74 meV (Fig. 2b4) is not due to the two abnormal data points near 73 meV (Fig. 2a4). By removing those two points, the effective bosonic spectral function extracted is similar to that obtained from the original data.
- [11] The spin excitation spectrum of LSCO $x=0.14$ shows a broad peak at a lower energy (~ 20 meV) (S. M. Hayden et al., Phys. Rev. Lett. **76**, 1344 (1996)). This peak is pushed down to below 5 meV in LSCO $x=0.07$ (H. Hiraka et al., J. Phys. Soc. Jpn **70**, 853 (2001)). A measurement from stripe ordered $\text{La}_{1.875}\text{Ba}_{0.125}\text{CuO}_4$ and related calculation showed a broad feature centered around 50~60 meV (Tranquada et al., cond-mat/0401621). Given that this is a different material at different doping, we do not consider this as relevant to the LSCO $x=0.03\sim 0.07$. The rapid change of spin spectra with doping has also been observed in $\text{YBa}_2\text{Cu}_3\text{O}_{7-\delta}$, S. Chakravarty et al., Phys. Rev. B **63**, 094503 (2001).
- [12] R. J. McQueeney et al., Phys. Rev. Lett. **87**, 077001 (2001); L. Pintschovious and M. Braden, Phys. Rev. B **60**, R15039 (1999).
- [13] Y. Ando et al., Phys. Rev. Lett. **87**, 017001 (2001).